MCB
Journals.ASM.org

Requisite Role for Nck Adaptors in Cardiovascular Development, Endothelial-to-Mesenchymal Transition, and Directed Cell Migration

Derek L. Clouthier,[a] Cameron N. Harris,[a] Richard A. Harris,[a] Claire E. Martin,[a] Mira C. Puri,[b] Nina Jones[a]

Department of Molecular and Cellular Biology, University of Guelph, Guelph, ON, Canada[a]; Lunenfeld-Tanenbaum Research Institute, Mount Sinai Hospital, and Department of Medical Biophysics, University of Toronto, Toronto, ON, Canada[b]

Development of the cardiovascular system is critically dependent on the ability of endothelial cells (ECs) to reorganize their intracellular actin architecture to facilitate migration, adhesion, and morphogenesis. Nck family cytoskeletal adaptors function as key mediators of actin dynamics in numerous cell types, though their role in EC biology remains largely unexplored. Here, we demonstrate an essential requirement for Nck within ECs. Mouse embryos lacking endothelial Nck1/2 expression develop extensive angiogenic defects that result in lethality at about embryonic day 10. Mutant embryos show immature vascular networks, with decreased vessel branching, aberrant perivascular cell recruitment, and reduced cardiac trabeculation. Strikingly, embryos deficient in endothelial Nck also fail to undergo the endothelial-to-mesenchymal transition (EnMT) required for cardiac valve morphogenesis, with loss of Nck disrupting expression of major EnMT markers, as well as suppressing mesenchymal outgrowth. Furthermore, we show that Nck-null ECs are unable to migrate downstream of vascular endothelial growth factor and angiopoietin-1, and they exhibit profound perturbations in cytoskeletal patterning, with disorganized cellular projections, impaired focal adhesion turnover, and disrupted actin-based signaling. Our collective findings thereby reveal a crucial role for Nck as a master regulator within the endothelium to control actin cytoskeleton organization, vascular network remodeling, and EnMT during cardiovascular development.

During embryogenesis, the cardiovascular system is the first organ system to develop, and it is established through several complex cellular processes involving embryonic endothelial cells (ECs). Coordinated cycles of EC proliferation, migration, and adhesion allow expansion of the primitive vascular network into a hierarchy of large and small vessels by the process of angiogenesis (1). Mesenchyme-derived pericytes and vascular smooth muscle cells (SMCs) are then recruited to nascent vessels, where they provide signals for vessel stabilization and maturation (2, 3). Development of the heart is also dependent on EC function, as endocardial ECs that line the primitive heart must undergo an endothelial-to-mesenchymal transition (EnMT) and invade the specialized extracellular matrix (ECM) known as the cardiac jelly (4). Here, they differentiate and contribute to the cardiac cushions, which are eventually remodeled into the valves and septa of the partitioned adult heart.

Assembly of a functional cardiovascular system is guided by molecular signal transduction pathways that mediate cross talk between ECs and surrounding support cells and ECM, via reorganization of the intracellular actin meshwork (5). Several classes of EC surface receptors, including the vascular endothelial growth factor receptor (VEGFR) and Tie receptor families, are essential for discrete phases of early cardiovascular development (6). In particular, Tie2 and VEGFR2 are principally implicated in the control of EC migration and adhesion during vascular morphogenesis through their ability to directly alter actin signaling (7). Upon ligand-induced activation of these receptors, autophosphorylation occurs on a specific set of tyrosine residues that serve as binding sites for signaling molecules containing Src homology 2 (SH2) domains (8), such as the Nck family of cytoskeletal adaptor proteins.

Nck proteins comprise a family of widely expressed intracellular adaptors with overlapping functions, consisting of Nck1/Nckα and Nck2/Nckβ/Grb4, and they have been identified to be key mediators of actin dynamics in several cell types, including kidney podocytes and spinal cord neurons (9, 10). In addition to an SH2 domain that can bind activated cell surface receptors, Nck proteins contain three Src homology 3 (SH3) domains which associate with a variety of downstream effector proteins that regulate cytoskeletal organization (11, 12). Interaction with the serine/threonine kinase Pak connects Nck to Rac-based cell motility pathways, while interaction with PINCH–integrin-linked kinase (ILK) complexes and focal adhesion kinase (FAK) allows Nck2 to bridge integrin and growth factor receptors, thereby affecting focal adhesion dynamics (13, 14). Nck also associates directly with neuronal WASp (N-WASp), leading to its localization and activation at the plasma membrane, binding of Arp2/3, and stimulation of actin polymerization (15–17). Within ECs, Nck has been shown to bind phosphotyrosine residues directly on VEGFR1 and -2 (18–20) as well as on Tie2 via the DokR scaffold protein (21), an interaction that promotes Pak-dependent cell migration (22). Several additional Nck-associated proteins have also been shown to be required for proper cardiovascular development, including FAK (23), ILK (24), and WAVE2 (25).

Although Nck has been implicated in several signaling pathways that regulate EC motility, a direct physiological role for Nck

Received 20 January 2015 **Returned for modification** 3 February 2015
Accepted 7 February 2015

Accepted manuscript posted online 17 February 2015

Citation Clouthier DL, Harris CN, Harris RA, Martin CE, Puri MC, Jones N. 2015. Requisite role for Nck adaptors in cardiovascular development, endothelial-to-mesenchymal transition, and directed cell migration. Mol Cell Biol 35:1573–1587. doi:10.1128/MCB.00072-15.

Address correspondence to Nina Jones, jonesmcb@uoguelph.ca.

D.L.C., C.N.H., and R.A.H. contributed equally to this article.

doi:10.1128/MCB.00072-15

in the endothelium has not yet been addressed. Previous studies have demonstrated that Nck adaptors are essential to the development of the embryo proper, as embryos lacking both Nck1 and Nck2 fail to survive beyond embryonic day 9.5 (E9.5) (26). However, the early lethality in these embryos precluded a detailed *in vivo* analysis of the cardiovascular system. In the study described here, we selectively inactivated *Nck* in ECs by employing the Cre/*loxP* system. In mouse embryos and primary cultured ECs, we show that Nck proteins function in the endothelium to regulate the dynamics of actin signaling, cell motility, EnMT, and angiogenesis, thereby establishing Nck signaling as an indispensable element of cardiovascular development.

MATERIALS AND METHODS

Mice and PCR genotyping. All work with transgenic laboratory mice was predefined under Animal Utilization Protocol 07R009, which was reviewed and sanctioned by the Animal Care Committee of the Senate Research Board, University of Guelph. The *Tie2-Cre* and *Nck1*$^{-/-}$ *Nck2*$^{flox/flox}$ (*Nck* double mutant [*NckDM*]) mouse lines were generously provided by Rong Wang (University of California at San Francisco, San Francisco, CA) and Tony Pawson (University of Toronto, Toronto, ON, Canada), respectively (23, 26), and Immortomouse mice were obtained from Charles River Laboratories. The mice were maintained in a mixed background and genotyped as described previously (9). Embryos were genotyped by PCR of genomic DNA prepared from embryonic tissue or the yolk sac. Genomic DNA was prepared by treating tissue with 75 μl of 25 mM NaOH and 0.2 mM disodium EDTA for 30 min at 95°C, followed by cooling to 4°C and addition of 75 μl of 40 mM Tris-HCl.

Whole-mount immunostaining. Embryos were harvested, and either yolk sacs or embryos were placed in 4% (vol/vol) paraformaldehyde (PFA) in PBS for 48 h at 4°C. Samples were dehydrated in subsequent 0, 25, 50, 80, and 100% methanol washes, and internal peroxidases were quenched in 2 ml of bleaching solution (methanol, dimethyl sulfoxide, and 30% hydrogen peroxide [Sigma-Aldrich] at 4:1:1, respectively) for 90 min at room temperature with rocking. Yolk sacs were then rehydrated with washes with 75%, 50%, and 25% methanol in phosphate-buffered saline (PBS) with 0.1% (vol/vol) Triton X-100 (PBT) for 5 min each at room temperature, followed by two washes with PBT for 30 min. For fluorescence staining, yolk sacs were blocked in 2 ml of blocking solution (2% skim milk in PBS, 2% Triton X-100, 0.2% bovine serum albumin [BSA; Sigma-Aldrich], 1% heat-inactivated goat serum [Fisher]) for 60 min at room temperature and then incubated with primary antibody (1:200 platelet endothelial cell adhesion molecule [PECAM]/CD31 [BD Pharmingen] or 1:200 smooth muscle actin [SMA; Sigma]) in blocking solution and incubated overnight at 4°C on a nutator. Samples were then placed in secondary antibody solution (1:400 goat anti-rat antibody—Alexa Fluor 488 [Invitrogen]) in blocking solution for 2 h at room temperature on a nutator, followed by three washes with PBT for 10 min at room temperature. Immunofluorescent images were taken using an upright multiphoton laser scanning confocal Leica DM 6000B microscope connected to a Leica TCS SP5 system and Leica LAS AF imaging software, as well as allied software provided by Becker and Hickl, according to the manufacturer's protocol. Nonfluorescent staining was achieved by the same methods listed above, but with a horseradish peroxidase (HRP)-conjugated secondary antibody (1:400 goat anti-rat antibody–HRP; BD Biosciences). Staining was performed using 3,3′-diaminobenzidine (Vector Laboratories) with nickel chloride, per the manufacturer's protocol.

Fluorescence immunostaining and quantitation. Paraffin sections 5 μm thick were adhered to slides and washed three times for 10 min each time in xylene, followed by sequential rehydration using ethanol washes, including a wash with a methanol–3% H_2O_2 solution to quench internal peroxidases and concluding with two 5-min washes in distilled water. Antigen retrieval was accomplished in Tris-EDTA solution for 20 min at 95°C, and then the samples were allowed to cool for 15 min before two 5-min washes in PBS containing 0.2% BSA and 0.1% Tween 20. Samples were blocked for 1 h in immunofluorescence buffer (PBS, 2% BSA, 2% fetal calf serum [FCS]) in a humidified chamber, washed in PBS, and then incubated with primary antibodies (VE-cadherin [catalog number ab33168; Abcam], SMA [catalog number A.2547; Sigma], S100A4 [catalog number ab27957; Abcam], claudin 5 [catalog number SC-28670; Santa Cruz], anti-Nckα [catalog number 07-099; Millipore], anti-Nckβ [catalog number 07-100; Millipore]) at a 1:200 dilution in blocking solution overnight at 4°C. Samples were then washed three times for 5 min each time in PBS with the appropriate secondary antibody (Alexa Fluor; Invitrogen), applied for 1 h at room temperature at a 1:400 dilution in blocking solution. Coverslips were mounted using ProLong Gold antifade reagent with DAPI (4′,6-diamidino-2-phenylindole; Life Technologies) and imaged on a Leica DMIRE2 microscope using a 20× objective lens, with Volocity software being used for image acquisition.

ImageJ software was used to quantify the staining intensity in DAPI-positive cells within the endocardial cushions. Using a 5-pixel tracing depth to outline either the endocardial or the myocardial regions, the intensity of both the marker stain and DAPI within each cushion was measured and expressed as a ratio.

Histological sectioning and hematoxylin and eosin staining. Histological sectioning and hematoxylin and eosin staining of embryos were performed by the Advanced Bioimaging Centre at Mount Sinai Hospital (Toronto, ON, Canada). Images were obtained using a Leica DM LB2 microscope and Leica Application Suite software following histological preparation.

Atrioventricular cushion explant culture. Timed matings between *Tie2-Cre*$^{+}$ males and *NckDM* females were established, with the morning of detection of a vaginal plug being defined as E0.5. Pregnant dams were euthanized using cervical dislocation, and embryos were harvested at E9.5 or E10.5 and somite matched (all were 21 to 25 or 32 to 38 somites, respectively) as previously reported (27). Atrioventricular canal (AVC) explants were established as previously described (28). The AVC and adjacent myocardium were carefully dissected from embryos under a Leica MZ12 dissecting microscope, explanted onto hydrated type I collagen gels (BD Biosciences), and allowed to adhere for 12 h. AVC explants were scored for mesenchymal cell invasion into the collagen matrix (<50 or >50 cells) by phase-contrast microscopy at 24 and 48 h using a Leica DMIRE2 microscope. Enumeration was conducted prior to determining the genotypes of the respective embryos to maintain objectivity.

Endothelial cell isolation and adenovirus infection. Primary and conditionally immortalized mouse lung endothelial cells (MLECs) were isolated from postnatal day 10 (P10) *NckDM* pups using the magnetic bead (Dynalbead M-450; Dynal Corporation) purification method with anti-mouse PECAM/CD31 antibody (BD Biosciences), as described previously (29, 30). MLECs were positively identified by their characteristic cobblestone morphology, via immunofluorescence microscopy with endothelial markers PECAM/CD31 (1:100; BD Biosciences) and CD102 (1:100; BD Biosciences) and via Western blot analysis (positive for endothelial marker VE-cadherin, negative for mesenchymal marker SMA). MLECs were cultured on 0.1% gelatin-coated (Sigma-Aldrich) polystyrene dishes in EC growth medium consisting of high-glucose Dulbecco's modified Eagle's medium (DMEM) supplemented with 20% (vol/vol) FCS, 100 U/ml penicillin, and 50 μg/ml streptomycin, with primary MLECs being further supplemented with 20 U/ml heparin, 1 mM nonessential amino acids, 1 mM sodium pyruvate, 0.5 μg/ml amphotericin B (Gibco), and 175 μg/ml EC growth supplement isolated from bovine neural tissue (Sigma-Aldrich). Primary MLECs were cultured at 37°C with 5% (vol/vol) CO_2. Conditionally immortalized MLECs were cultured at 33°C and switched to 37°C at least 3 days prior to the experiments to facilitate inactivation of large T antigen.

Type 5 recombinant adenoviruses in which E1 and E3 were deleted and whose genomes encoded the Cre recombinase (Adeno-Cre) or green fluorescent protein (GFP) control (Adeno-GFP) were purchased from

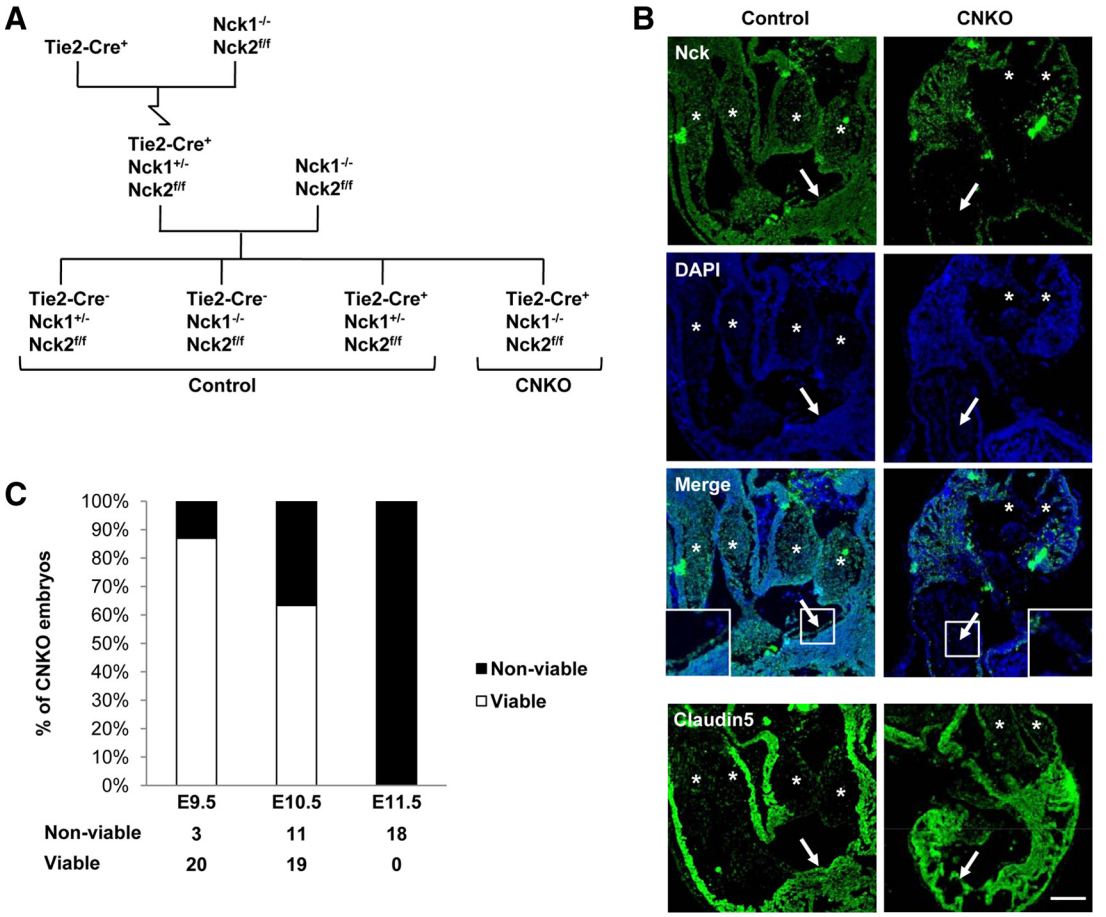

FIG 1 Generation and characterization of embryos lacking Nck expression in endothelial cells. (A) Breeding strategy used to generate conditional CNKO embryos with Nck deleted in the embryonic endothelium. The mutant genotype is *Tie2-Cre*$^{+}$ *Nck1*$^{-/-}$ *Nck2*$^{flox/flox}$ (Nck2^{ff}), and control genotypes are collectively *Tie2-Cre*$^{-}$ *Nck1*$^{+/-}$ *Nck2*$^{flox/flox}$, *Tie2-Cre*$^{-}$ *Nck1*$^{-/-}$ *Nck2*$^{flox/flox}$, and *Tie2-Cre*$^{+}$ *Nck1*$^{+/-}$ *Nck2*$^{flox/flox}$. (B) The efficiency of Cre-mediated *Nck2* excision specifically within the vasculature of E10.5 CNKO embryos is shown via immunohistochemical analysis of Nck expression. Nck (green) is observed in the cardiac cushions (asterisks) and endocardial layer (arrows) of control but not CNKO embryos. (Insets) Images of the boxed areas highlighting the loss of Nck staining exclusively within the CNKO endocardium. Residual staining in CNKO embryos represents nonendothelial expression of Nck2. Cells are highlighted using DAPI (blue). (Bottom row) An adjacent section showing the endothelial marker claudin 5. Bar, 100 μm. (C) Proportion of viable versus nonviable CNKO embryos at E9.5, E10.5, and E11.5, as determined by the presence versus the absence of a heartbeat. The loss of endothelial Nck results in embryonic lethality between E10 and E11.

Vector Biolabs. Infection of MLECs was performed as previously described by our group for mouse embryonic fibroblasts (31). A multiplicity of infection of 500 was used for MLECs, and no detectable toxicity was observed. Adenovirus-infected MLECs were used by at least 72 h postinfection, with Nck2 deletion being confirmed by Western blotting and immunostaining.

Western blotting. Lysates were prepared from MLEC cultures following adenovirus infection using phospholipase C lysis buffer supplemented with fresh protease inhibitors (leupeptin and aprotinin), sodium pervanadate, and phenylmethylsulfonyl fluoride (9). The primary antibodies used were anti-Nck (1:500; catalog number 610100; BD Biosciences), anti-FAK (1:1,000; catalog number 04-591; Millipore), anti-FAK pY397 (1:1,000; catalog number 05-1140; Millipore), anti-Rac1 (1:1,000; catalog number 05-389; Millipore), anti-RhoA (1:1,000; catalog number sc-418; Santa Cruz), β-actin (1:5,000; catalog number A1978; Sigma), and anti-GAPDH (anti-glyceraldehyde-3-phosphate dehydrogenase; 1:1,000; catalog number G041; Applied Biological Materials Inc.). Nck1- and Nck2-specific antibodies (1:1,000) were a kind gift from Louise Larose (McGill University, Montreal, QC, Canada) (32).

GTPase activation assays. Glutathione beads bound to glutathione *S*-transferase (GST)–Pak1 (for active Rac1 pulldown) or GST-rhotekin (for active RhoA pulldown) (both from Cytoskeleton Inc.) were incubated for 1 h at 4°C with 500 μg of lysate from uninfected (no adenovirus) or Adeno-Cre-infected MLECs. Cells had been serum starved for 24 h prior to stimulation with 100 ng/ml Ang1 or vascular endothelial growth factor (VEGF) (both from Peprotech) for 15 min at 37°C. The beads were then washed three times, and eluted proteins were subject to Western blot analysis. Densitometry was performed on a ChemiDoc XRS+ imaging system (Bio-Rad), and data were analyzed using ImageLab software (Bio-Rad). The proportion of active Rac1 or RhoA present within each treatment was determined as the ratio of the signal in the pulldown versus that in the input lysate samples.

Wound closure cell migration assay. The wound closure assay was performed as previously described by others (33). Uninfected (no adenovirus), Adeno-Cre-infected, or Adeno-GFP-infected primary MLECs were plated on 0.1% sterile gelatin-coated dishes and serum starved for at least 24 h. Confluent cultures were then wounded with a sterile micropipette tip, and serum-free DMEM with 100 ng/ml angiopoietin-1 (Ang1) or VEGF (both from Peprotech) was added. Cultures were imaged at consistent locations at 0, 2, 6, 12, 18, and 24 h. Images were acquired using a Leica DMIRE2 microscope and Leica CTR MIC camera.

Boyden chamber cell migration assay. Cell migration assays were performed using 24-well Transwell inserts (Corning). Primary MLECs

TABLE 1 Genotypic frequency of embryos

Stage	No. of litters	No. of embryos				Total
		Tie2-Cre^{-} *Nck1*$^{+/-}$ *Nck2*$^{flox/flox}$	*Tie2-Cre*$^{-}$ *Nck1*$^{-/-}$ *Nck2*$^{flox/flox}$	*Tie2-Cre*$^{+}$ *Nck1*$^{+/-}$ *Nck2*$^{flox/flox}$	*Tie2-Cre*$^{+}$ *Nck1*$^{-/-}$ *Nck2*$^{flox/flox}$	
E9.5	7	21	20	17	23[a]	81
E10.5	10	21	26	26	30[a]	103
E11.5	4	15	20	13	18[a]	66
P21	11	31	24	24	0	79

[a] Some embryos were found dead; see Fig. 1C for details.

were serum starved for 24 h and then trypsinized and subsequently treated with a trypsin inhibitor isolated from *Glycine max* (Sigma-Aldrich) to avoid adding serum. Cells (1×10^5) were added to the upper well, and the bottom well contained either 100 ng/ml Ang1 or murine VEGF (both from Peprotech) in serum-free DMEM with 100 U/ml penicillin and 50 μg/ml streptomycin. After 6 h of incubation at 37°C with 5% (vol/vol) CO_2, cells were fixed in 4% (vol/vol) PFA in PBS for 15 min at room temperature, rinsed, stained with modified Meyer's hematoxylin, and imaged under an upright Leica DM1000 scope. The cells within 10 random high-power fields were enumerated, and experiments were performed in triplicate.

Cell adhesion and spreading assays. Adeno-Cre- and Adeno-GFP-infected MLECs were trypsinized and plated on coverslips coated with 0.1% sterile gelatin in DMEM supplemented with 10% FCS, 100 U/ml penicillin, and 50 μg/ml streptomycin. Slides were fixed in 4% (vol/vol) PFA in PBS for 15 min at room temperature. Samples were then fluorescently immunostained with Nck2 (1:100; Abcam), Texas Red phalloidin (1:40; Invitrogen), and/or paxillin (1:50; Santa Cruz) in PBS. Slides were fixed in DAPI ProLong Gold mounting medium (Invitrogen). Samples were observed under a Leica DMIRE2 epifluorescence microscope, and the cell surface area was quantified using ImageJ freeware.

Proliferation assay. Adeno-Cre- and Adeno-GFP-infected MLECs were trypsinized and counted such that 5,000 cells were plated per well in triplicate on a 96-well plate with 100 μl of medium. Cells were allowed to adhere for 12 h prior to addition of 100 μl of 0.05 mM resazurin blue (Sigma). Plates were incubated at 37°C in 5% CO_2, and the fluorescence was measured 4 h later (designated time zero) on a BioTek FLX100 microplate reader. Similar measurements were taken at 24-h intervals for 96 h. The fold change was calculated by dividing the fluorescence reading at each time point by that at time zero for each condition.

Statistics. Comparisons between treatments and biological groups were achieved by employing a one-way analysis of variance with the Tukey-Kramer multiple-comparison test with data assumed to be sampled from populations that follow Gaussian distributions. Statistical significance is indicated in the appropriate figures and figure legends. The statistical software used was Prism (version 6; GraphPad).

RESULTS

Endothelial cell-specific *Nck* deletion in mice results in embryonic lethality. To investigate the role of Nck expression during cardiovascular development, mice expressing Cre recombinase under the control of the endothelial cell-enriched *Tie2* promoter and enhancer were intercrossed with mice homozygous for the *Nck1*-null allele (*Nck1*$^{-/-}$) and homozygous for a floxed allele of *Nck2* (*Nck2*$^{flox/flox}$), to facilitate deletion of Nck2 in embryonic

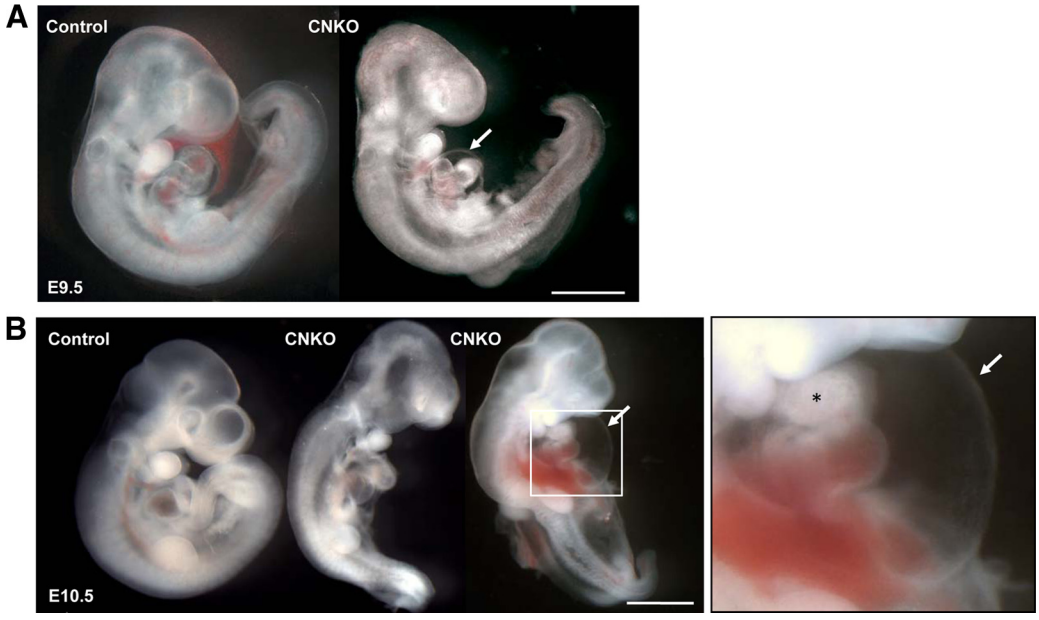

FIG 2 Conditional deletion of *Nck* in the endothelium results in embryonic lethality. Representative whole-mount images of control and CNKO embryos at E9.5 and E10.5 are shown. (A) At E9.5, CNKO embryos show underdevelopment of the heart, characterized by a reduced heart size, abnormal looping, and dilation of the pericardial cavity (arrow) compared to the findings for control embryos. (B) By E10.5, CNKO embryos are smaller than those of their control littermates, with hemorrhage and blood congestion being found throughout the body. The image on the right is an enlarged image of the boxed area highlighting severe pericardial edema (arrow) and disrupted cardiac chamber formation (asterisk). Bars, 1 mm.

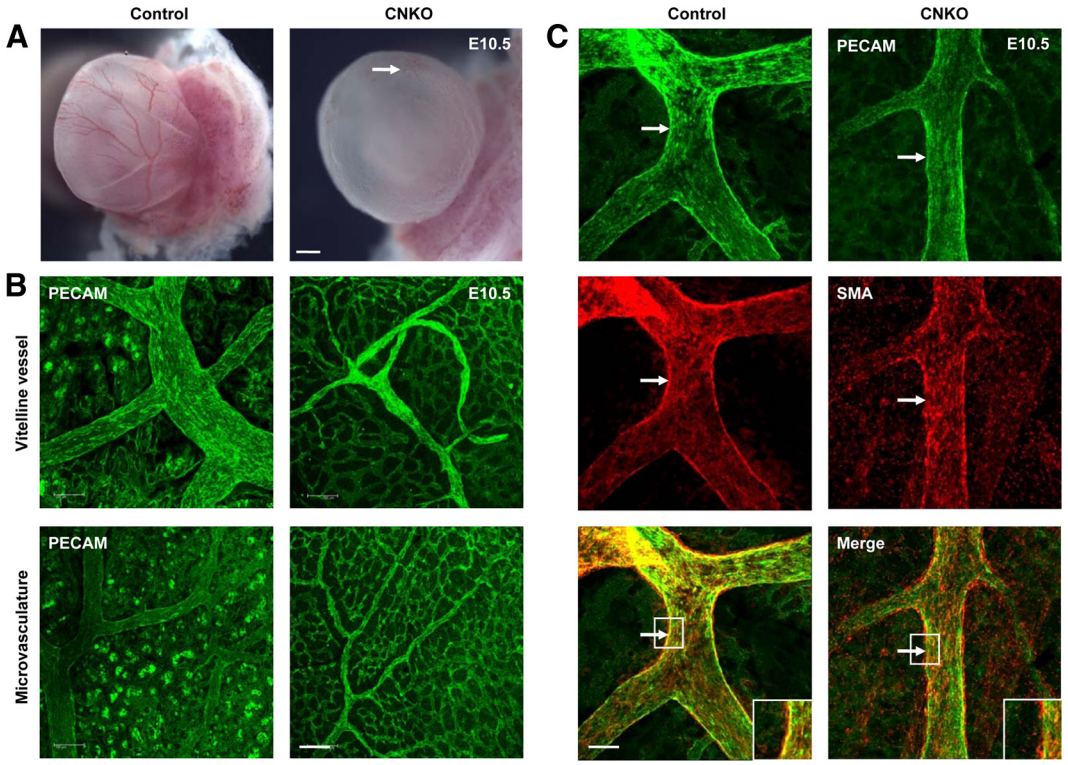

FIG 3 CNKO yolk sacs exhibit decreased vessel remodeling and vessel integrity. (A) At E10.5, the yolk sacs of CNKO embryos appear pale in comparison to those of control embryos, owing to the underdevelopment of major and minor vessels (arrow). Bar, 1 mm. (B) Immunofluorescent PECAM staining of E10.5 yolk sacs demonstrates the reduced caliber of the vitelline vessel in CNKO yolk sacs compared to that of the controls, as well as poorly remodeled microvascular networks. Bar, 100 μm. (C) Dual immunofluorescence staining of E10.5 yolk sacs with PECAM and SMA shows an altered recruitment and association of smooth muscle cells with the vitelline vessel and major branches in CNKO yolk sacs compared to the findings for the controls (arrows and insets). Bar, 100 μm.

endothelial cells of Nck1-null mice (Fig. 1A). Only male *Tie2-Cre*$^{+}$ mice were used in breedings, as *Tie2* regulatory sequences have been reported to drive the expression of Cre in the female germ line, thus resulting in global gene deletion (34). Of the viable offspring obtained at weaning ($n = 79$), none were of the mutant conditional *Nck*-knockout (CNKO) genotype, and the remaining three control genotypes of *Tie2-Cre*$^{-}$ *Nck1*$^{+/-}$ *Nck2*$^{flox/flox}$, *Tie2-Cre*$^{-}$ *Nck1*$^{-/-}$ *Nck2*$^{flox/flox}$, and *Tie2-Cre*$^{+}$ *Nck1*$^{+/-}$ *Nck2*$^{flox/flox}$ were observed at approximately equal frequencies (Table 1). This suggests that Nck1 and Nck2 have overlapping and mutually compensatory functions within the endothelium and that the loss of Nck expression therein during mouse development results in embryonic lethality.

To determine the precise developmental time point at which CNKO embryos succumb to lethality, timed matings were set up and embryos were analyzed at gestational ages of E9.5 to E11.5. All four possible genotypes were represented with a normal Mendelian frequency of approximately 25% (Table 1). Loss of Nck expression specifically within the endothelium was confirmed via Nck immunostaining on E10.5 embryos, using antibodies that recognize both Nck1 and Nck2 (Fig. 1B). The presence or absence of a heartbeat was used to assess whether the embryos were alive or nonviable. By E11.5, no CNKO embryos had a heartbeat, whereas 63% of E10.5 CNKO embryos and 87% of E9.5 CNKO embryos had a heartbeat (Fig. 1C). At E9.5, the majority of CNKO embryos were similar to those of their control littermates, though CNKO embryos occasionally displayed pericardial edema, abnormal heart looping, and a reduced heart size (Fig. 2A). By E10.5, CNKO embryos were noticeably smaller than their control littermates, and there were obvious developmental defects in the heart, head, and neural tube regions, as well as the corresponding yolk sacs (Fig. 2B and 3A). Specifically, most E10.5 CNKO embryos showed a reduction in head size as well as dilation of the pericardium and fewer heartbeats (Fig. 2B). Blood was present within major arteries and the heart, although in both E9.5 and E10.5 CNKO embryos, hemorrhage and blood congestion could be observed within various locations throughout the body (Fig. 2A and B). By E11.5, the CNKO embryos were markedly smaller than their littermates and showed extensive tissue deterioration throughout the body (data not shown). There were no observable differences among the non-CNKO control embryos, and all were viable. Together these results suggest that the CNKO embryos succumb to lethality between E10 and E11.

Widespread vascular defects exist within CNKO yolk sacs and embryos. The extent of vascular perfusion of the yolk sac was readily apparent in freshly dissected embryos. At E10.5, control yolk sacs had a well-developed vascular tree with a thick vitelline vessel and numerous other large vessels (Fig. 3A). In contrast, CNKO yolk sacs were pale with a poorly defined vasculature, although blood perfusion was still evident (Fig. 3A). Immunofluorescent whole-mount microscopy using the EC marker anti-PECAM (also known as CD31) revealed that the major vitelline vessel and surrounding large vessels of the CNKO yolk sacs had formed but were of much lower caliber than the vessels of control

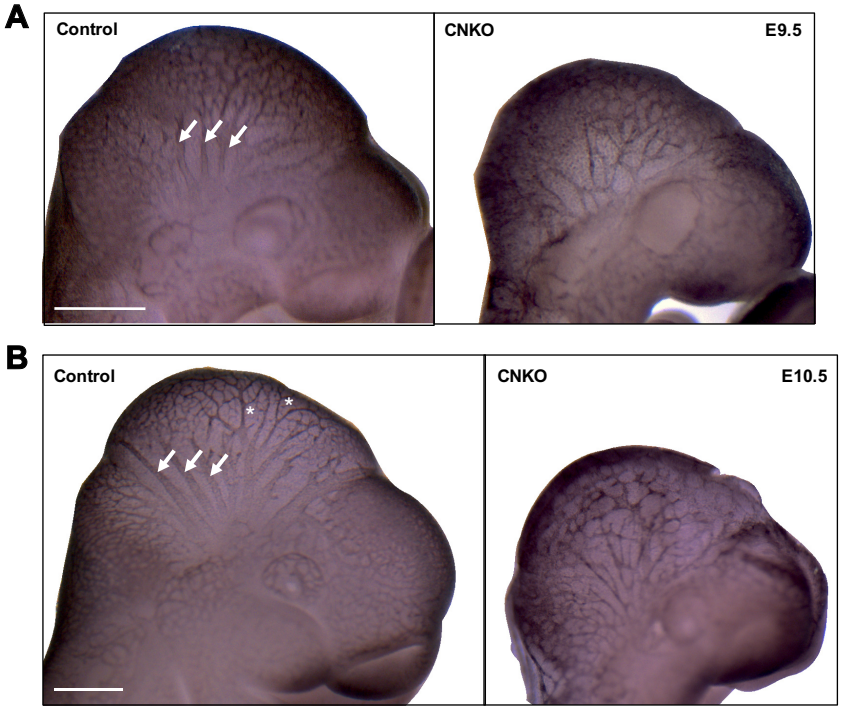

FIG 4 Defects in vascular remodeling in CNKO embryos. Whole-mount immunostaining of control and CNKO embryos for PECAM at E9.5 (20 to 25 somites) (A) or E10.5 (31 to 38 somites) (B). Control embryos show large-caliber major vessels in the head (arrows) at E9.5 with extensive branching (asterisks) by E10.5, while cranial vessels are underdeveloped and poorly organized in CNKO embryos. The images shown are representative of those for 14 embryos at E9.5 and 8 embryos at E10.5 for controls and of those for 5 embryos at E9.5 and 3 embryos at E10.5 for CNKO embryos. Bars, 500 μm (A) and 250 μm (B).

littermate embryos (Fig. 3B). In areas of microvasculature networks, control yolk sacs displayed a hierarchical pattern of remodeled large and small vessels, whereas the microvessels in the CNKO yolk sacs were more uniform in size (Fig. 3B). Furthermore, these vessels remained associated with the surrounding honeycomb-like primary capillary plexus, which had already regressed by this time point in the control yolk sacs, thereby indicating a failure to remodel the yolk sac vasculature in the absence of endothelial Nck expression. To next examine the structural integrity of the CNKO yolk sac vessels, we performed double immunofluorescence staining with PECAM and smooth muscle actin (SMA) antibodies to visualize ECs and support cells, respectively. At E10.5, which is the time point at which SMC progenitors begin to invest the vessel wall (35), SMCs were readily detected to be surrounding the major vitelline vessel wall of both the control and CNKO yolk sacs (Fig. 3C). However, compared to the uniform organization of SMCs in the embryos of their control littermates, a discontinuous staining pattern was observed in the CNKO yolk sac vitelline vessel, such that the SMCs did not appear to be properly aligned along the vessel wall (Fig. 3C). These results suggest a defect in reciprocal signaling between ECs and the newly recruited SMCs in CNKO embryos.

To visualize EC patterning in the embryo proper, we performed whole-mount anti-PECAM-1 immunostaining on E9.5 and E10.5 embryos. At E9.5 and E10.5, control embryos exhibited highly organized vascular network formation in the developing head region, with a hierarchy of large and small branches extending from major cephalic vessels (Fig. 4). In addition, several branched vessels extended from the dorsal aorta between somites, and along the midline of the embryo, an extensive perineural vascular plexus formed in control embryos (data not shown). In contrast, at E9.5 and E10.5 the CNKO embryos showed severe defects in both the degree of vessel branching and the organization of the vascular networks of the head and between somites, with underdeveloped major vessels and a chaotic vascular network being found (Fig. 4 and data not shown). Taken together, these results reveal an essential role for the Nck adaptor proteins in ECs during angiogenic remodeling and vascular maturation.

Inactivation of Nck in endothelium results in defects in myocardial trabeculation and endocardial cushion formation. To examine the cardiac defects in more detail, histological analysis of CNKO and control embryos was performed on E10.5. Control heart sections revealed a continuous endocardial lining along both the ventricular and atrial chambers, and trabeculated myocardium within the ventricle could also be seen (Fig. 5). These sections also showed prominent bulges consistent with endocardial cushions between the myocardium and endocardial lining (Fig. 5). In contrast, sections from CNKO hearts indicated a discontinuous endocardial lining with a thin myocardium and reduced trabeculation (Fig. 5). The CNKO heart sections also showed a dramatic reduction in size, organization, and cellularity of the endocardial cushions in the atrioventricular canal (AVC) and outflow tract (OT) (Fig. 5). Nck expression in the endothelium is therefore essential for proper heart development.

Endothelial Nck expression is required for EnMT. Previous studies have established that formation of the endocardial cushions is dependent on endothelial-to-mesenchymal transition (EnMT) (reviewed in reference 36). One hallmark of EnMT is the

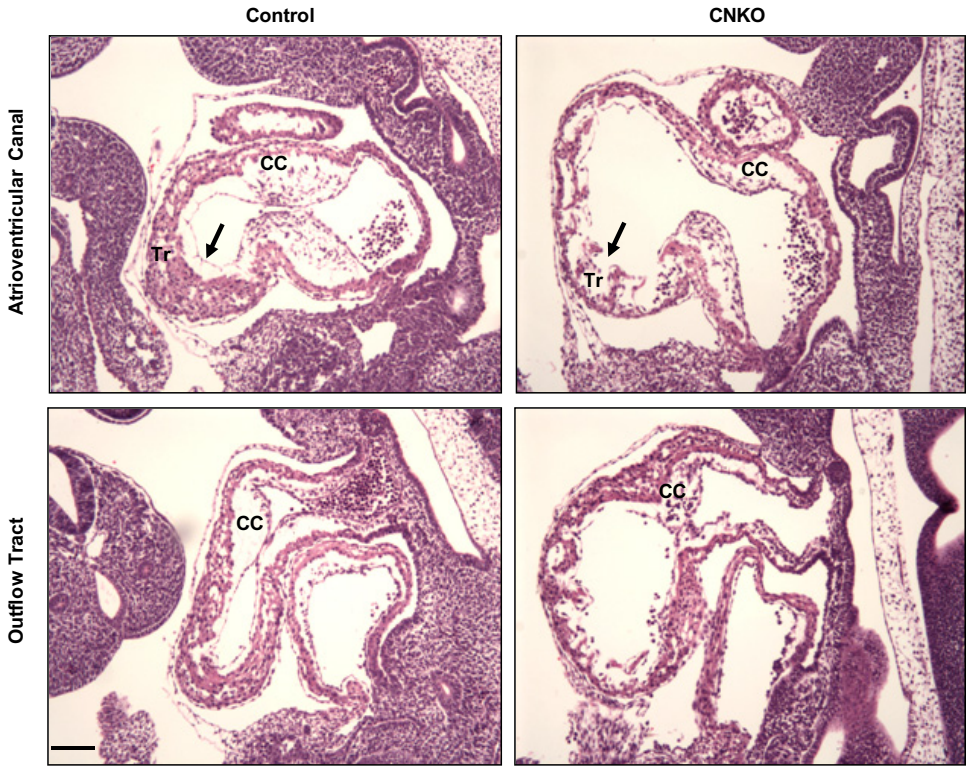

FIG 5 Characterization of cardiac defects in CNKO embryos. Hematoxylin-and-eosin-stained sagittal sections of control and CNKO embryos at E10.5 show the atrioventricular canal and outflow tract of the developing heart. CNKO embryos show a discontinuous endocardial lining (arrows), as well as reduced myocardial trabeculation (Tr), compared to the findings for the controls. Also, the well-defined cardiac cushions (CC) seen in the control embryos are hypoplastic in the CNKO embryos. Bar, 100 μm.

downregulation of endothelial markers and upregulation of mesenchymal markers (37). To further characterize the endocardial cushion defect observed in CNKO embryos, we performed fluorescent immunohistology of several molecular markers of EnMT at E10.5, a time point at which EnMT is complete in the normal mouse embryo. Staining of E10.5 embryos revealed a significantly higher intensity of the endothelial markers VE-cadherin and claudin 5 within the AVC of CNKO embryos than within the AVC of control embryos (Fig. 6A and B). In contrast, CNKO embryos displayed reduced levels of the mesenchymal markers S100A4 (also known as fibroblast-specific protein 1 [FSP1]) and SMA within the AVC compared to their control littermates (Fig. 6A and B). Taken together, CNKO embryos showed aberrant retention of endothelial markers and failed to express mesenchymal markers within the AVC, thereby confirming that the loss of Nck within the endothelium disrupts the molecular program that induces EnMT.

A second hallmark of EnMT is the acquisition of migratory and invasive properties. Between E9.5 and E10.5, the endocardium responds to signals from the myocardium, instructing the cells to lose cell-cell contacts and adopt an elongated morphology, allowing subsequent invasion and migration through the underlying ECM (cardiac jelly). To validate the potential requirement for Nck during EnMT, we next employed an *ex vivo* endocardial cushion explant assay, in which mesenchymal cells grow out from microdissected AVCs and invade a three-dimensional collagen matrix akin to cardiac jelly (28). At E9.5, a time point marking the onset of EnMT, AVC explants from control or CNKO embryos were cultured on hydrated type I collagen gels, and mesenchymal outgrowth was quantified by viewing explant cultures under a phase-contrast microscope at 24 and 48 h following plating (Fig. 6C). After 24 h, 30% of control explants and 0% of CNKO explants had >50 cells growing out into the collagen gel (Fig. 6D). By 48 h, ~80% of the control explants and ~20% of the CNKO explants had >50 cell outgrowths (Fig. 6D). At both times at which the cells were evaluated, cells from control explants that had migrated into the collagen gels exhibited a mesenchymal morphology with several cytoplasmic projections. In contrast, outgrowths from the CNKO explants had fewer and ill-defined cell projections that simply grew longer and into the collagen gels with time. Both control and CNKO endocardial cushion explants successfully adhered to the collagen gels at approximately similar proportions (80% and 82%, respectively). Endocardial cells from CNKO embryos therefore show a marked reduction in migration and invasion, highlighting a role for Nck in normal mesenchyme formation in the developing heart.

Defective cell migration in response to proangiogenic growth factors in Nck-null endothelial cells. Our finding that embryos lacking Nck expression in ECs display severe defects in cardiovascular development, including EnMT and sprouting angiogenesis, prompted us to investigate whether this might be due to defective cell migration processes. To this end, we isolated and cultured primary mouse lung ECs (MLECs) from *Nck1*$^{-/-}$ *Nck2*$^{flox/flox}$ mice. In parallel, we established immortalized MLECs following intercrossing of *Nck1*$^{-/-}$ *Nck2*$^{flox/flox}$ mice with Immortomouse mice. To delete *Nck2* from *Nck1*-null MLECs, cultures were transduced with recombinant type 5 adenovirus encoding

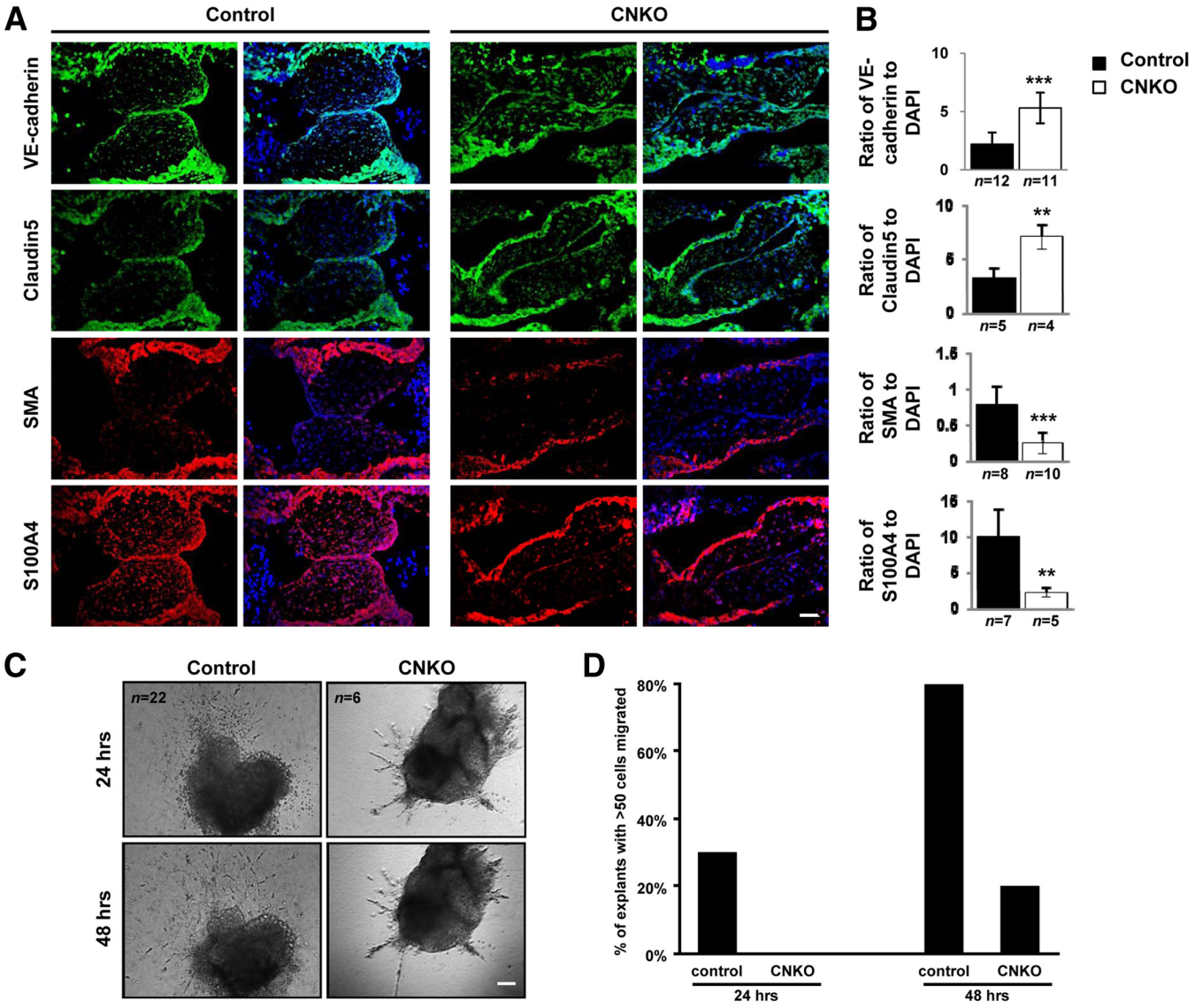

FIG 6 CNKO embryos show altered EnMT. (A) Immunofluorescent analysis of the endothelial markers VE-cadherin and claudin 5 (both green) and mesenchymal markers S100A4 and SMA (both red) within the AVC in serial sections obtained from E10.5 control and CNKO embryos, using DAPI (blue) counterstain. Bar, 50 μm. (B) Quantitative analysis of EnMT markers shows increased expression of VE-cadherin and claudin 5 and decreased expression of S100A4 and SMA in CNKO embryos compared to their levels of expression in the controls. The number of embryos analyzed is indicated below each histogram bar. **, $P < 0.01$; ***, $P < 0.0001$. (C) Phase-contrast images of AVC explants from E9.5 control or CNKO embryos at 24 and 48 h after plating on a collagen matrix. Bar, 100 μm. (D) Quantitative analysis of EnMT in AVC explants shows decreased cell outgrowth from CNKO explants compared to that for the controls at both time points. Individual explants were scored according to whether greater than or fewer than 50 cells had migrated into the collagen gels after plating.

Cre recombinase (Adeno-Cre) or GFP (Adeno-GFP) or left untreated (no adenovirus). Western blot analysis shows the efficiency of Nck2 deletion in Adeno-Cre-infected MLECs, while Nck2 expression remained in Adeno-GFP-infected and uninfected control cells (Fig. 7A and B). We then used these cells to examine whether the loss of Nck would affect the migration mediated by Tie2 and VEGFR2, as signaling by these receptor tyrosine kinases plays a central role in EC motility. Primary MLECs were subjected to a wound closure assay in the presence or absence of Tie2-activating ligand Ang1 or VEGF. After 24 h, both Ang1 and VEGF induced the nearly complete closure of Adeno-GFP-infected MLEC scratch wounds, while Adeno-Cre-infected MLECs displayed reduced wound closure, even in the presence of Ang1 or VEGF (Fig. 7C).

To better quantify the effect of Nck on EC migration in response to proangiogenic signaling, we performed Boyden chamber assays using Ang1 and VEGF. Primary MLECs infected with Adeno-GFP exhibited increased migration in response to Ang1 and VEGF compared to the overall migration under conditions without chemoattractant (Fig. 7D). In contrast, MLECs infected with Adeno-Cre showed a significant decrease in migration potential under all conditions compared to that of Adeno-GFP-infected cells (Fig. 7D). Interestingly, VEGF stimulation was able to produce a modest yet significant increase in cell migration in Adeno-Cre-infected MLECs compared to that with no chemoattractant, but this effect was not seen with Ang1 (Fig. 7D). We further verified that these migration defects were not simply due to differences in the proliferation rate between MLECs with or without

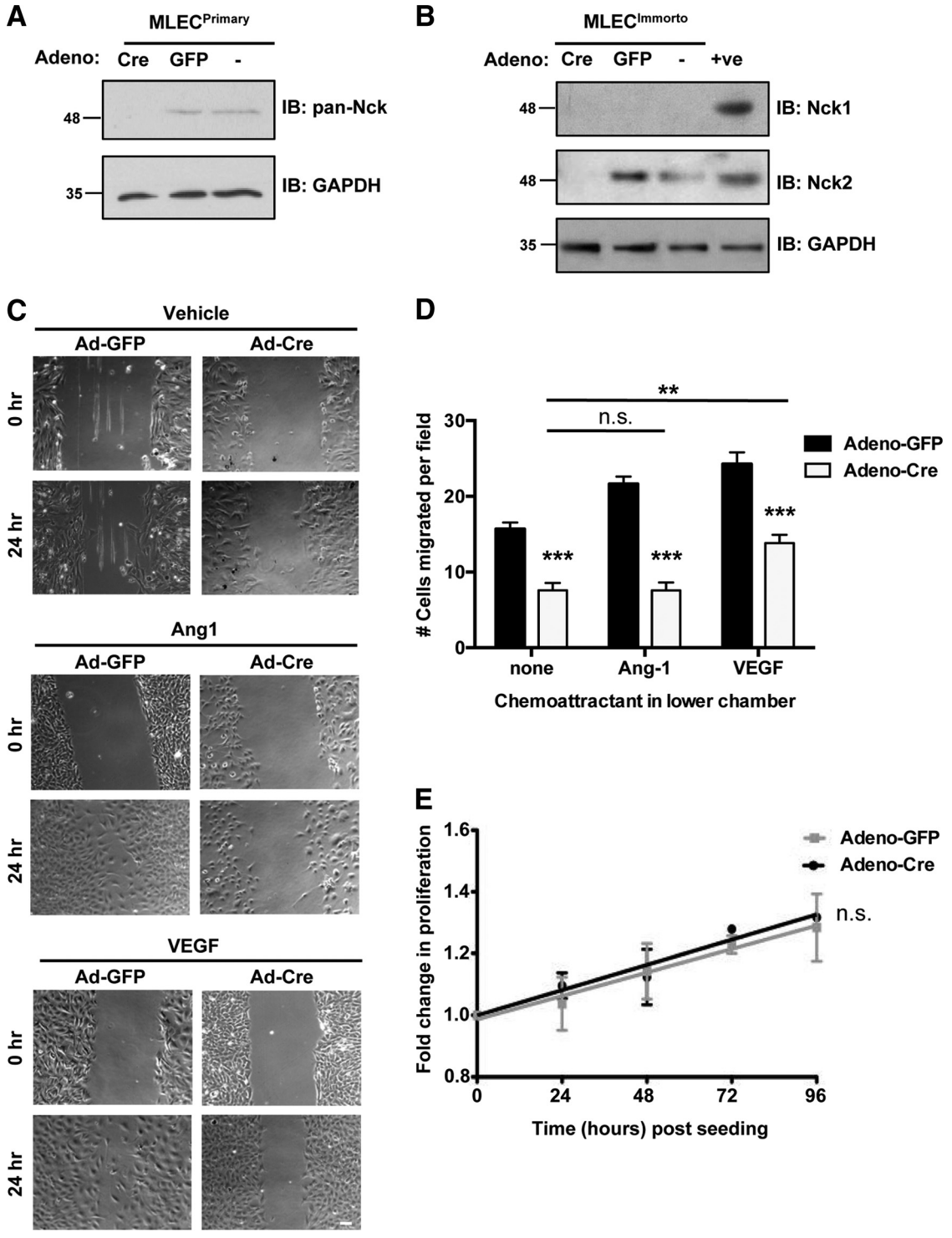

FIG 7 Endothelial cells lacking Nck display defects in directed cell migration. (A) Immunoblots (IBs) of lysates obtained from primary MLECs transduced with Adeno-GFP or Adeno-Cre or left uninfected (−), showing a loss of Nck protein expression specifically within Adeno-Cre-infected cells (first lane). GAPDH shows equal protein loading of all MLEC samples. (B) Western blots of lysates obtained from conditionally immortalized MLECs transduced with Adeno-GFP or Adeno-Cre or left uninfected (−), showing that specific Cre-mediated Nck2 deletion results in the complete absence of Nck proteins (first lane). +ve, positive control. In panels A and B, numbers to the left of the blots are molecular masses (in kilodaltons). (C) Wound closure assay on confluent monolayers of primary MLECs transduced with either Adeno-GFP or Adeno-Cre and cultured on gelatin in the presence or absence of Ang1 or VEGF. Images of the same fields were taken at 0 and 24 h after wounding, and those shown are representative of the images from three independent experiments. Adeno-Cre-infected cells showed reduced wound closure under all conditions tested. Bar, 70 μm. (D) Boyden chamber assay on primary MLECs transduced with either Adeno-GFP or Adeno-Cre using either 100 ng/ml Ang1, 100 ng/ml VEGF, or no stimulus. The cells within at least seven random high-power fields were enumerated, and experiments were performed in triplicate. Adeno-Cre-infected cells showed a highly significant reduction ($P < 0.001$) in migration compared to Adeno-GFP-infected cells under all conditions tested, though a modest yet significant increase ($P < 0.01$) in migration of Adeno-Cre-infected cells could be seen with addition of VEGF compared to that seen with no chemoattractant. **, $P < 0.01$; ***, $P < 0.0001$; n.s., nonsignificant. (E) Proliferation assay on immortalized MLECs transduced with either Adeno-GFP or Adeno-Cre showing a nonsignificant difference in the growth rate in the presence or absence of Nck. Each time point represents data for 9 assays.

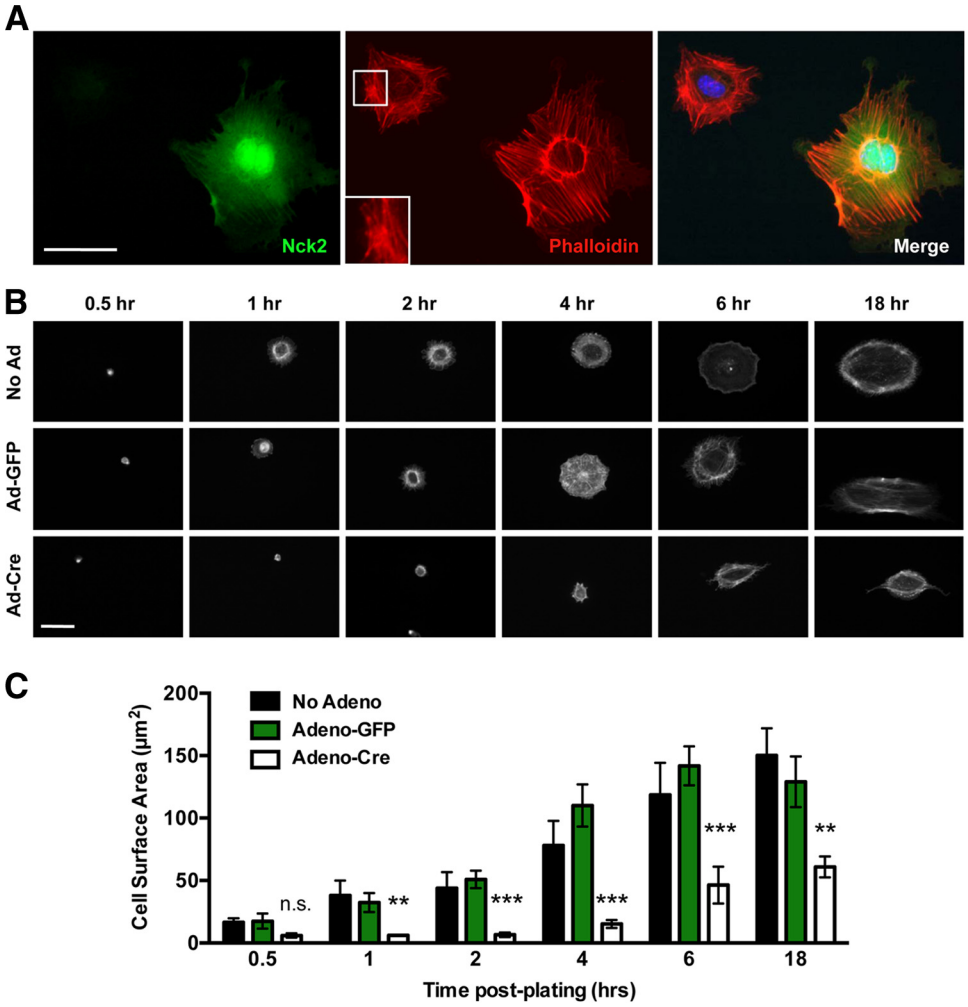

FIG 8 Altered actin organization and decreased cell spreading within Nck-deficient endothelial cells. (A) Representative fluorescence micrographs from a pool of Adeno-Cre-infected primary MLECs stained with anti-Nck2 antibodies (green), fluorescent phalloidin to show the morphology of F actin (red), and DAPI to highlight the position of the nucleus position (blue). Prominent parallel stress fibers and lamellipodial protrusions can be seen in Nck-expressing cells, while Nck-deficient MLECs are smaller, with stress fibers appearing short, disorganized, and highly bundled (inset). Bar, 30 μm. (B) Time course images of phalloidin-stained MLECs from panel A following 0.5, 1, 2, 4, 6, and 18 h of spreading on 0.1% gelatin-coated coverslips. Cells were simultaneously immunostained with Nck antibodies to confirm *Nck2* excision. Adeno-Cre-infected MLECs show a reduced cell size with an altered actin morphology. Bar, 30 μm. (C) Quantitation of the results shown in panel B demonstrating that Adeno-Cre infection results in decreased cell spreading in comparison to that for Adeno-GFP-infected and uninfected (No Adeno) control cells. The histogram represents the mean cell surface area ± SEM for a minimum 6 to 10 cells per replicate. **, $P < 0.01$; ***, $P < 0.0001$; n.s., nonsignificant.

Nck expression (Fig. 7E). Together, these studies indicate that directed EC motility is impaired in the absence of Nck adaptors and that Nck in ECs is required within angiogenic signaling pathways induced by Ang1 as well as VEGF.

Endothelial cells lacking Nck show defects in actin organization, cell spreading, and focal adhesion remodeling in response to proangiogenic stimuli. As EC motility is facilitated by signaling pathways that regulate actin polymerization, we next sought to determine whether the absence of the Nck adaptor proteins might induce alterations in the EC actin cytoskeleton. Adeno-Cre-infected primary MLECs were stained with fluorescent phalloidin, to monitor the morphology of the actin cytoskeleton, in addition to Nck, to confirm cell-specific Cre-based excision of *Nck2*. Compared to the findings for noninfected neighboring cells expressing Nck2, which possessed well-defined lamellipodia and peripheral actin spikes, MLECs devoid of Nck lacked substantial lamellipodia and extended short, haphazardly organized projections (Fig. 8A). Furthermore, the cells exhibited a loss of stress fiber uniformity and were smaller. These findings led us to question whether similar abnormalities would be observed during cell spreading, which involves dynamic actin remodeling. Adeno-GFP-transduced and nontransduced cells showed very similar patterns of spreading: by 1 h postseeding, both cell types established lamellipodia as well as prominent radial stress fibers that extended into the periphery (Fig. 8B). In contrast, Adeno-Cre-infected MLECs lacked distinct lamellipodia until 18 h postseeding and developed fractal-like protrusions rather than symmetric radial projections (Fig. 8B), which likely contributed to the delayed spreading and, ultimately, the reduced surface area observed in these cells (Fig. 8C).

Lastly, we examined the induction of stress fibers as well as the organization of focal adhesions in immortalized MLECs in response to Ang1 and VEGF stimulation. Similar to observations

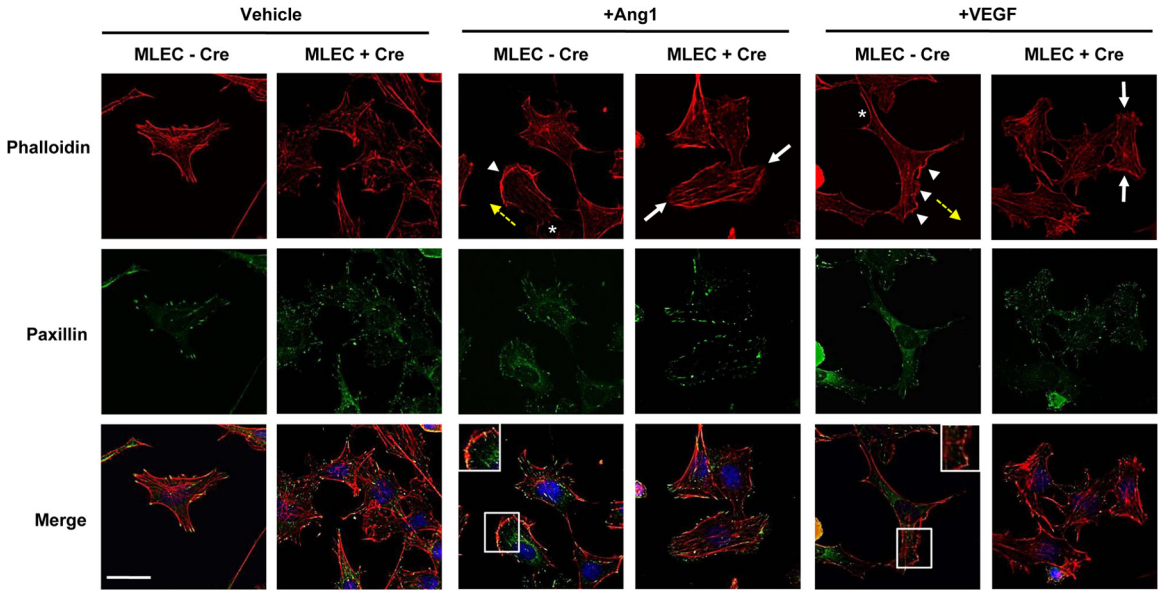

FIG 9 Aberrant focal adhesion remodeling in response to angiogenic stimuli in Nck-null MLECs. Representative fluorescence micrographs from immortalized MLECs that were transduced with Adeno-Cre (+Cre) or left uninfected (−Cre) and treated with 100 ng/ml Ang1 or 100 ng/ml VEGF for 15 min or vehicle alone. Fixed cells were stained with antipaxillin antibodies to highlight focal adhesion structures (green), fluorescent phalloidin to show the morphology of F actin (red), and DAPI to indicate the position of the nucleus (blue). Paxillin staining is found throughout the interior and periphery of unstimulated Nck-deficient MLECs, whereas it localizes exclusively to the periphery of control cells. Upon stimulation with Ang1 or VEGF, control cells assembled robust unidirectional lamellipodia (arrowheads) in the direction of cell movement (yellow arrows) which were accompanied by posterior stress fibers (asterisks), and focal adhesion structures were restricted to the tips of these projections (insets on merged images). In contrast, processes extended in multiple directions in Cre-infected cells (white arrows), and focal adhesions appeared larger, with paxillin punctae being localized around the entire cell periphery. Bar, 30 μm.

in primary MLECs, unstimulated Nck-deficient immortalized MLECs were smaller than control cells and lacked oriented stress fibers (Fig. 9, Vehicle). Notably, a diffuse interior accumulation of punctae representing the focal adhesion protein paxillin was also observed in Cre-infected (+Cre) cells, while punctae representing paxillin in uninfected control (−Cre) cells were organized at the periphery at stress fiber tips (Fig. 9, Vehicle). Upon stimulation with Ang1, control cells displayed a clear polarized morphology, characterized by the assembly of robust unidirectional lamellipodia and filopodia which were accompanied by posterior stress fibers, and focal adhesion structures were localized to the tips of these projections, consistent with their migratory phenotype (Fig. 9, +Ang1). In contrast, lamellipodia and filopodia extended in multiple directions in Cre-infected cells stimulated with Ang1, and intriguingly, large focal adhesions appeared to encircle the entire cell periphery (Fig. 9, +Ang1), suggesting that altered focal adhesion disassembly could underlie the defect in migration seen under these conditions. Stimulation with VEGF produced a similar, albeit less pronounced effect (Fig. 9, +VEGF), in keeping with the ability of VEGF to weakly induce migration in Nck-deficient MLECs (Fig. 7D). Collectively, these studies demonstrate that Nck plays a critical role in the organization and dynamic remodeling of the EC cytoskeletal network.

Endothelial Nck deficiency alters Rho GTPase activity and FAK signaling. To explore the mechanistic basis for altered actin remodeling and focal adhesion formation associated with Nck deficiency, we investigated the signaling properties of immortalized MLECs in response to angiogenic stimuli. Given the central role of FAK activation in promoting focal adhesion turnover (38), we first examined its autophosphorylation following treatment with Ang1 or VEGF. We noted a striking decrease in FAK phosphorylation on the major site Y397 in Cre-infected MLECs under both treatment conditions compared to that in control cells (Fig. 10A to C), consistent with the unusually mature appearance of focal adhesion structures in these cells following growth factor stimulation. Next, we investigated whether aberrant activation of Rho family GTPases, which function as molecular switches to facilitate changes in cell shape and motility, might contribute to this phenotype. Using standard GST pulldown assays, we found decreased activity of RhoA and increased activity of Rac1 following Ang1 stimulation in Cre-infected MLECs compared to their activities in control cells (Fig. 10D to F). Similar findings of decreased RhoA activity and increased Rac1 activity were obtained upon VEGF stimulation (Fig. 10G to I). The extent of FAK and GTPase activation was comparable in unstimulated cells with or without Cre transduction (Fig. 10A and data not shown). These results regarding RhoA and Rac1 support our prior observations of fewer stress fibers and an increased frequency of lamellar protrusions, respectively, in Ang1 or VEGF-stimulated Nck-deficient MLECs (Fig. 9). Together, our findings reveal defects in core signaling pathways required for cell migration, adhesion, and EnMT in the absence of Nck expression, thereby underscoring the role of Nck as an essential organizer in ECs during cardiovascular development.

DISCUSSION

In this study, we have determined that deletion of the Nck family of adaptor proteins within the endothelium leads to defective angiogenic remodeling, resulting in impaired cardiovascular development and embryonic lethality at about E10.5. This phenotype is strikingly similar to that observed in the absence of Tie2 or Ang1, including the simplified head and intersomitic vasculature and reduced cardiac trabeculation (39, 40). Additionally, perivascular cell recruitment is similarly perturbed, as seen in the disorganized

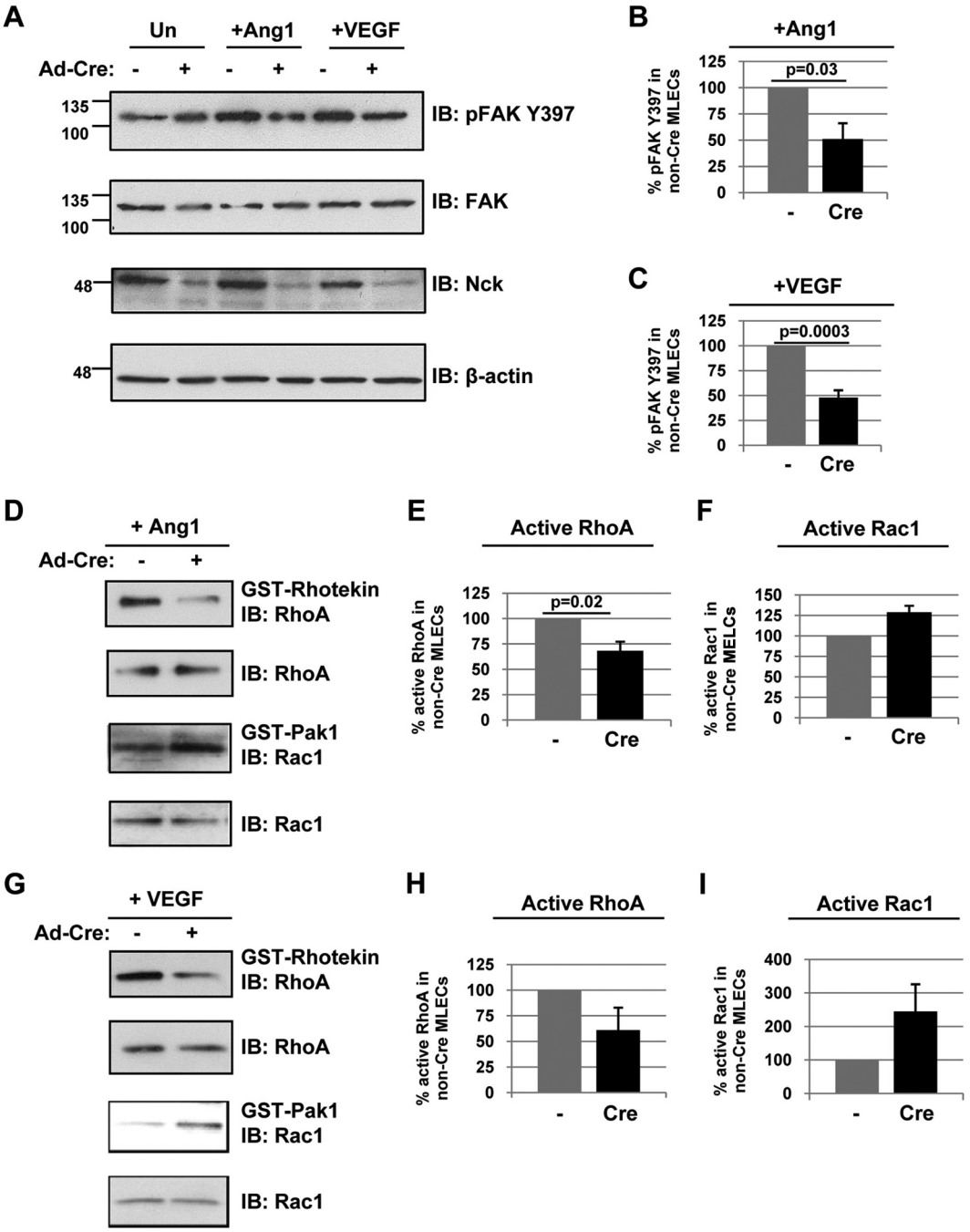

FIG 10 Endothelial Nck deficiency alters Rho GTPase and FAK activation. (A to C) Lysates obtained from immortalized MLECs (with or without Cre transduction) were treated with 100 ng/ml Ang1 or VEGF for 15 min and immunoblotted with antibodies recognizing pFAK Y397, FAK, Nck, or β-actin. Densitometric quantitation of the results in panel A demonstrates a significant decrease in FAK activation in Nck-null MLECs in response to Ang1 (B) and VEGF (C). β-Actin shows equal protein loading of all MLEC samples, and specific deletion of Nck upon Adeno-Cre transduction can also be observed. Results shown are representative of those from three to five independent experiments. In panel A, the numbers to the left of the blots are molecular masses (in kilodaltons). (D to I) Parallel lysates from panel A were incubated with GST-rhotekin or GST-Pak1 and immunoblotted with antibodies recognizing RhoA or Rac1. Densitometric quantitation of the results in panels D and G demonstrates a decrease in RhoA activation in Nck-null MLECs in response to Ang1 (E) and VEGF (H) and an increase in Rac1 activation in Nck-null MLECs in response to Ang1 (F) and VEGF (I). The relative amount of active Rac1 or RhoA in the Cre-transduced MLECs is represented as the percentage of the amount of active Rac1 or RhoA in control cells. Results are representative of those from three independent experiments.

myocardial layering, impaired SMC investment in the yolk sac vasculature, and widespread hemorrhaging. Tie2 kinase activity is critically important for its function (39), and it has been hypothesized that the DokR-Nck binding site on phosphorylated Tie2 contributes to vascular stability by facilitating aspects of reciprocal signaling between ECs and Ang1-expressing SMCs which lead to SMC recruitment and attachment (41). Accordingly, our *in vivo* observations coupled with our *in vitro* findings that Nck-null

MLECs show defective cell adhesion and morphology imply that indirect binding of Nck to Tie2 contributes to the maintenance of EC shape, allowing proper SMC attachment and vessel maturation (42).

We also provide evidence that implicates Nck in the developmental process of EnMT, which is central to heart valve morphogenesis. EnMT has been further hypothesized to play a role in vessel sprouting by enabling directional migration of specialized ECs known as tip cells at the angiogenic front (37). While it is possible that the defects observed in CNKO embryos are a result of reduced hemodynamic forces acting to remodel the developing heart (43), our collective results provide evidence for a direct role of Nck during EnMT. First, via immunoanalysis of the cardiac cushion regions, we found that CNKO embryos were unable to properly acquire the mesenchymal cell marker SMA or S100A4 or lose the endothelial cell marker VE-cadherin or claudin 5. Second, in an *ex vivo* AVC explant assay, we demonstrated that the loss of endothelial Nck impaired mesenchymal outgrowth. Lastly, the *in vitro* migration assays verified the defect in cell motility in Nck-deficient ECs. Nck may thus be required to first direct ECs to the appropriate location for formation of the cushion structures and subsequently allow the completion of transformation to mesenchymal cells.

Interestingly, several Nck-associated signaling molecules have also been linked to mesenchymal transformation, including FAK and the Rho GTPase family of downstream effectors. Correspondingly, we identified defects in regulation of these proteins in Nck-null ECs, including decreased FAK phosphorylation, decreased RhoA activity, and increased Rac1 activity. FAK and its autophosphorylation on Y397 are required for expression and stabilization of the transcription factor Snail (44), which is a major regulator of the epithelial-to-mesenchymal transition (45). Of note, it has been proposed that many of the cytoskeletal defects in FAK-null cells may in fact be due to altered mesenchymal lineage commitment (44), and given the similar phenotypes of embryos lacking Nck and FAK in ECs, it is plausible that Nck could exert a comparable effect. The small GTPases RhoA, Rac1, and Cdc42 are all regulated by Nck signaling (46, 47), and coordinated activation of these proteins is a common element in the switch to a mesenchymal phenotype. Activation of RhoA is intimately linked to the increased expression of SMA (48), as well as the phosphorylation events on claudin 5 that lead to its internalization (49). Similarly, opposing actions of RhoA and Rac1 also lead to VE-cadherin internalization (50), thereby reducing cell adhesion and promoting the acquisition of mesenchymal characteristics (51). Lastly, RhoA is required for activation of STAT transcription factors (52), which can in turn upregulate S100A4 expression and thus influence mesenchymal transformation (53). Taken together, our data provide a putative molecular mechanism to allow retention of endothelial markers and failure to acquire mesenchymal markers during valve morphogenesis in the CNKO embryos.

We have further determined that ECs lacking Nck expression display alterations in actin cytoskeleton organization, having a reduced capacity to spread and migrate in response to VEGF and Ang1. These phenotypes are accompanied by profound defects in stress fiber formation, cell polarity, focal adhesion turnover, and regulation of FAK, RhoA, and Rac1. Our findings complement those of Rivera and colleagues, who employed short hairpin RNA-mediated knockdown of Nck in human umbilical vein endothelial cells and live-cell microscopy to elegantly establish a mechanism by which Nck guides cell polarization and the stabilization of cell-substrate adhesions to facilitate directional cell migration (54). We now extend this model *in vivo* to propose that in the context of angiogenic sprouting, Nck further modulates the function of endothelial tip cells and other ECs, allowing them to physically extend from the leading edge of nascent vessels and guide their movement in response to chemotactic gradients of growth factors (55).

In summary, the results presented here clearly identify Nck to be a critical adaptor protein during cardiovascular development, and its central role in cytoskeletal signaling and motility downstream of proangiogenic factors underscores its potential significance in the broad range of diseases manifesting altered angiogenesis and EnMT.

ACKNOWLEDGMENTS

We thank Rong Wang (University of California at San Francisco, San Francisco, CA) and Tony Pawson and Julie Ruston (Samuel Lunenfeld Research Institute, Toronto, ON, Canada) for sharing mouse lines and expertise and Louise Larose (McGill University, Montreal, QC, Canada) for kindly providing Nck antibodies. We also acknowledge Ken Harpal (Mount Sinai Hospital, Toronto, ON, Canada) for assistance with embryo sectioning and Dan Dumont (Sunnybrook Research Institute, Toronto, ON, Canada) as well as members of the N. Jones laboratory for helpful comments on the manuscript. We are also grateful to Martha Smith and the University of Guelph Central Animal Facility staff for their assistance with animal maintenance.

This work was supported by an operating grant from the Canadian Institutes of Health Research (MOP number 93526) and an Early Researcher Award (to N.J.). N.J. is the recipient of a Natural Sciences and Engineering Research Council (NSERC) University Faculty Award and a New Investigator Award from the Kidney Research Scientist Core Education and National Training (KRESCENT) Program and is a Tier 2 Canada Research Chair.

REFERENCES

1. **Carmeliet P.** 2003. Blood vessels and nerves: common signals, pathways and diseases. Nat Rev Genet **4:**710–720. http://dx.doi.org/10.1038/nrg1158.
2. **Carmeliet P.** 2000. Mechanisms of angiogenesis and arteriogenesis. Nat Med **6:**389–395. http://dx.doi.org/10.1038/74651.
3. **Armulik A, Abramsson A, Betsholtz C.** 2005. Endothelial/pericyte interactions. Circ Res **97:**512–523. http://dx.doi.org/10.1161/01.RES.0000182903.16652.d7.
4. **Srivastava D, Olson EN.** 2000. A genetic blueprint for cardiac development. Nature **407:**221–226. http://dx.doi.org/10.1038/35025190.
5. **Adams RH, Alitalo K.** 2007. Molecular regulation of angiogenesis and lymphangiogenesis. Nat Rev Mol Cell Biol **8:**464–478. http://dx.doi.org/10.1038/nrm2183.
6. **Jones N, Iljin K, Dumont DJ, Alitalo K.** 2001. Tie receptors: new modulators of angiogenic and lymphangiogenic responses. Nat Rev Mol Cell Biol **2:**257–267. http://dx.doi.org/10.1038/35067005.
7. **Lamalice L, Le Boeuf F, Huot J.** 2007. Endothelial cell migration during angiogenesis. Circ Res **100:**782–794. http://dx.doi.org/10.1161/01.RES.0000259593.07661.1e.
8. **Pawson T.** 2004. Specificity in signal transduction: from phosphotyrosine-SH2 domain interactions to complex cellular systems. Cell **116:**191–203. http://dx.doi.org/10.1016/S0092-8674(03)01077-8.
9. **Jones N, Blasutig IM, Eremina V, Ruston JM, Bladt F, Li H, Huang H, Larose L, Li SS, Takano T, Quaggin SE, Pawson T.** 2006. Nck adaptor proteins link nephrin to the actin cytoskeleton of kidney podocytes. Nature **440:**818–823. http://dx.doi.org/10.1038/nature04662.
10. **Fawcett JP, Georgiou J, Ruston J, Bladt F, Sherman A, Warner N, Saab BJ, Scott R, Roder JC, Pawson T.** 2007. Nck adaptor proteins control the organization of neuronal circuits important for walking. Proc Natl Acad Sci U S A **104:**20973–20978. http://dx.doi.org/10.1073/pnas.0710316105.
11. **Li W, Fan J, Woodley DT.** 2001. Nck/Dock: an adapter between cell

surface receptors and the actin cytoskeleton. Oncogene **20:**6403–6417. http://dx.doi.org/10.1038/sj.onc.1204782.
12. **Buday L, Wunderlich L, Tamas P.** 2002. The Nck family of adapter proteins: regulators of actin cytoskeleton. Cell Signal **14:**723–731. http://dx.doi.org/10.1016/S0898-6568(02)00027-X.
13. **Tu Y, Li F, Goicoechea S, Wu C.** 1999. The LIM-only protein PINCH directly interacts with integrin-linked kinase and is recruited to integrin-rich sites in spreading cells. Mol Cell Biol **19:**2425–2434.
14. **Goicoechea SM, Tu Y, Hua Y, Chen K, Shen TL, Guan JL, Wu C.** 2002. Nck-2 interacts with focal adhesion kinase and modulates cell motility. Int J Biochem Cell Biol **34:**791–805. http://dx.doi.org/10.1016/S1357-2725(02)00002-X.
15. **Eden S, Rohatgi R, Podtelejnikov AV, Mann M, Kirschner MW.** 2002. Mechanism of regulation of WAVE1-induced actin nucleation by Rac1 and Nck. Nature **418:**790–793. http://dx.doi.org/10.1038/nature00859.
16. **Higgs HN, Pollard TD.** 1999. Regulation of actin polymerization by Arp2/3 complex and WASp/Scar proteins. J Biol Chem **274:**32531–32534. http://dx.doi.org/10.1074/jbc.274.46.32531.
17. **Rohatgi R, Nollau P, Ho HY, Kirschner MW, Mayer BJ.** 2001. Nck and phosphatidylinositol 4,5-bisphosphate synergistically activate actin polymerization through the N-WASP-Arp2/3 pathway. J Biol Chem **276:**26448–26452. http://dx.doi.org/10.1074/jbc.M103856200.
18. **Igarashi K, Isohara T, Kato T, Shigeta K, Yamano T, Uno I.** 1998. Tyrosine 1213 of Flt-1 is a major binding site of Nck and SHP-2. Biochem Biophys Res Commun **246:**95–99. http://dx.doi.org/10.1006/bbrc.1998.8578.
19. **Stoletov KV, Ratcliffe KE, Spring SC, Terman BI.** 2001. NCK and PAK participate in the signaling pathway by which vascular endothelial growth factor stimulates the assembly of focal adhesions. J Biol Chem **276:**22748–22755. http://dx.doi.org/10.1074/jbc.M009720200.
20. **Lamalice L, Houle F, Huot J.** 2006. Phosphorylation of Tyr1214 within VEGFR-2 triggers the recruitment of Nck and activation of Fyn leading to SAPK2/p38 activation and endothelial cell migration in response to VEGF. J Biol Chem **281:**34009–34020. http://dx.doi.org/10.1074/jbc.M603928200.
21. **Jones N, Dumont DJ.** 1998. The Tek/Tie2 receptor signals through a novel Dok-related docking protein, Dok-R. Oncogene **17:**1097–1108. http://dx.doi.org/10.1038/sj.onc.1202115.
22. **Master Z, Jones N, Tran J, Jones J, Kerbel RS, Dumont DJ.** 2001. Dok-R plays a pivotal role in angiopoietin-1-dependent cell migration through recruitment and activation of Pak. EMBO J **20:**5919–5928. http://dx.doi.org/10.1093/emboj/20.21.5919.
23. **Braren R, Hu H, Kim YH, Beggs HE, Reichardt LF, Wang R.** 2006. Endothelial FAK is essential for vascular network stability, cell survival, and lamellipodial formation. J Cell Biol **172:**151–162. http://dx.doi.org/10.1083/jcb.200506184.
24. **Friedrich EB, Liu E, Sinha S, Cook S, Milstone DS, MacRae CA, Mariotti M, Kuhlencordt PJ, Force T, Rosenzweig A, St-Arnaud R, Dedhar S, Gerszten RE.** 2004. Integrin-linked kinase regulates endothelial cell survival and vascular development. Mol Cell Biol **24:**8134–8144. http://dx.doi.org/10.1128/MCB.24.18.8134-8144.2004.
25. **Yamazaki D, Suetsugu S, Miki H, Kataoka Y, Nishikawa S, Fujiwara T, Yoshida N, Takenawa T.** 2003. WAVE2 is required for directed cell migration and cardiovascular development. Nature **424:**452–456. http://dx.doi.org/10.1038/nature01770.
26. **Bladt F, Aippersbach E, Gelkop S, Strasser GA, Nash P, Tafuri A, Gertler FB, Pawson T.** 2003. The murine Nck SH2/SH3 adaptors are important for the development of mesoderm-derived embryonic structures and for regulating the cellular actin network. Mol Cell Biol **23:**4586–4597. http://dx.doi.org/10.1128/MCB.23.13.4586-4597.2003.
27. **Nomura-Kitabayashi A, Anderson GA, Sleep G, Mena J, Karabegovic A, Karamath S, Letarte M, Puri MC.** 2009. Endoglin is dispensable for angiogenesis, but required for endocardial cushion formation in the midgestation mouse embryo. Dev Biol **335:**66–77. http://dx.doi.org/10.1016/j.ydbio.2009.08.016.
28. **Camenisch TD, Molin DG, Person A, Runyan RB, Gittenberger-de Groot AC, McDonald JA, Klewer SE.** 2002. Temporal and distinct TGF-beta ligand requirements during mouse and avian endocardial cushion morphogenesis. Dev Biol **248:**170–181. http://dx.doi.org/10.1006/dbio.2002.0731.
29. **Cattelino A, Liebner S, Gallini R, Zanetti A, Balconi G, Corsi A, Bianco P, Wolburg H, Moore R, Oreda B, Kemler R, Dejana E.** 2003. The conditional inactivation of the beta-catenin gene in endothelial cells causes a defective vascular pattern and increased vascular fragility. J Cell Biol **162:**1111–1122. http://dx.doi.org/10.1083/jcb.200212157.
30. **Peng X, Ueda H, Zhou H, Stokol T, Shen TL, Alcaraz A, Nagy T, Vassalli JD, Guan JL.** 2004. Overexpression of focal adhesion kinase in vascular endothelial cells promotes angiogenesis in transgenic mice. Cardiovasc Res **64:**421–430. http://dx.doi.org/10.1016/j.cardiores.2004.07.012.
31. **Hawley SP, Wills MK, Jones N.** 2010. Adenovirus-mediated genetic removal of signaling molecules in cultured primary mouse embryonic fibroblasts. J Vis Exp **2010:**2160. http://dx.doi.org/10.3791/2160.
32. **Latreille M, Laberge MK, Bourret G, Yamani L, Larose L.** 2011. Deletion of Nck1 attenuates hepatic ER stress signaling and improves glucose tolerance and insulin signaling in liver of obese mice. Am J Physiol Endocrinol Metab **300:**E423–E434. http://dx.doi.org/10.1152/ajpendo.00088.2010.
33. **Shen TL, Park AY, Alcaraz A, Peng X, Jang I, Koni P, Flavell RA, Gu H, Guan JL.** 2005. Conditional knockout of focal adhesion kinase in endothelial cells reveals its role in angiogenesis and vascular development in late embryogenesis. J Cell Biol **169:**941–952. http://dx.doi.org/10.1083/jcb.200411155.
34. **de Lange WJ, Halabi CM, Beyer AM, Sigmund CD.** 2008. Germ line activation of the Tie2 and SMMHC promoters causes noncell-specific deletion of floxed alleles. Physiol Genomics **35:**1–4. http://dx.doi.org/10.1152/physiolgenomics.90284.2008.
35. **Majesky MW, Dong XR, Regan JN, Hoglund VJ.** 2011. Vascular smooth muscle progenitor cells: building and repairing blood vessels. Circ Res **108:**365–377. http://dx.doi.org/10.1161/CIRCRESAHA.110.223800.
36. **Armstrong EJ, Bischoff J.** 2004. Heart valve development: endothelial cell signaling and differentiation. Circ Res **95:**459–470. http://dx.doi.org/10.1161/01.RES.0000141146.95728.da.
37. **Potenta S, Zeisberg E, Kalluri R.** 2008. The role of endothelial-to-mesenchymal transition in cancer progression. Br J Cancer **99:**1375–1379. http://dx.doi.org/10.1038/sj.bjc.6604662.
38. **Huveneers S, Danen EH.** 2009. Adhesion signaling—crosstalk between integrins, Src and Rho. J Cell Sci **122:**1059–1069. http://dx.doi.org/10.1242/jcs.039446.
39. **Dumont DJ, Gradwohl G, Fong GH, Puri MC, Gertsenstein M, Auerbach A, Breitman ML.** 1994. Dominant-negative and targeted null mutations in the endothelial receptor tyrosine kinase, tek, reveal a critical role in vasculogenesis of the embryo. Genes Dev **8:**1897–1909. http://dx.doi.org/10.1101/gad.8.16.1897.
40. **Suri C, Jones PF, Patan S, Bartunkova S, Maisonpierre PC, Davis S, Sato TN, Yancopoulos GD.** 1996. Requisite role of angiopoietin-1, a ligand for the TIE2 receptor, during embryonic angiogenesis. Cell **87:**1171–1180. http://dx.doi.org/10.1016/S0092-8674(00)81813-9.
41. **Tachibana K, Jones N, Dumont DJ, Puri MC, Bernstein A.** 2005. Selective role of a distinct tyrosine residue on Tie2 in heart development and early hematopoiesis. Mol Cell Biol **25:**4693–4702. http://dx.doi.org/10.1128/MCB.25.11.4693-4702.2005.
42. **Patan S.** 1998. TIE1 and TIE2 receptor tyrosine kinases inversely regulate embryonic angiogenesis by the mechanism of intussusceptive microvascular growth. Microvasc Res **56:**1–21. http://dx.doi.org/10.1006/mvre.1998.2081.
43. **Lucitti JL, Jones EA, Huang C, Chen J, Fraser SE, Dickinson ME.** 2007. Vascular remodeling of the mouse yolk sac requires hemodynamic force. Development **134:**3317–3326. http://dx.doi.org/10.1242/dev.02883.
44. **Li XY, Zhou X, Rowe RG, Hu Y, Schlaepfer DD, Ilic D, Dressler G, Park A, Guan JL, Weiss SJ.** 2011. Snail1 controls epithelial-mesenchymal lineage commitment in focal adhesion kinase-null embryonic cells. J Cell Biol **195:**729–738. http://dx.doi.org/10.1083/jcb.201105103.
45. **Yang Z, Rayala S, Nguyen D, Vadlamudi RK, Chen S, Kumar R.** 2005. Pak1 phosphorylation of snail, a master regulator of epithelial-to-mesenchyme transition, modulates snail's subcellular localization and functions. Cancer Res **65:**3179–3184. http://dx.doi.org/10.1158/0008-5472.CAN-04-3480.
46. **Ruusala A, Pawson T, Heldin CH, Aspenstrom P.** 2008. Nck adapters are involved in the formation of dorsal ruffles, cell migration, and Rho signaling downstream of the platelet-derived growth factor beta receptor. J Biol Chem **283:**30034–30044. http://dx.doi.org/10.1074/jbc.M800913200.
47. **Guan S, Fan J, Han A, Chen M, Woodley DT, Li W.** 2009. Non-compensating roles between Nckalpha and Nckbeta in PDGF-BB signaling to promote human dermal fibroblast migration. J Invest Dermatol **129:**1909–1920. http://dx.doi.org/10.1038/jid.2008.457.
48. **Mihira H, Suzuki HI, Akatsu Y, Yoshimatsu Y, Igarashi T, Miyazono K, Watabe T.** 2012. TGF-beta-induced mesenchymal transition of MS-1 endothelial cells requires Smad-dependent cooperative activation of Rho

signals and MRTF-A. J Biochem **151:**145–156. http://dx.doi.org/10.1093/jb/mvr121.

49. **Shen W, Li S, Chung SH, Zhu L, Stayt J, Su T, Couraud PO, Romero IA, Weksler B, Gillies MC.** 2011. Tyrosine phosphorylation of VE-cadherin and claudin-5 is associated with TGF-beta1-induced permeability of centrally derived vascular endothelium. Eur J Cell Biol **90:**323–332. http://dx.doi.org/10.1016/j.ejcb.2010.10.013.
50. **Mammoto T, Parikh SM, Mammoto A, Gallagher D, Chan B, Mostoslavsky G, Ingber DE, Sukhatme VP.** 2007. Angiopoietin-1 requires p190 RhoGAP to protect against vascular leakage in vivo. J Biol Chem **282:**23910–23918. http://dx.doi.org/10.1074/jbc.M702169200.
51. **Lampugnani MG, Zanetti A, Breviario F, Balconi G, Orsenigo F, Corada M, Spagnuolo R, Betson M, Braga V, Dejana E.** 2002. VE-cadherin regulates endothelial actin activating Rac and increasing membrane association of Tiam. Mol Biol Cell **13:**1175–1189. http://dx.doi.org/10.1091/mbc.01-07-0368.
52. **Pelletier S, Duhamel F, Coulombe P, Popoff MR, Meloche S.** 2003. Rho family GTPases are required for activation of Jak/STAT signaling by G protein-coupled receptors. Mol Cell Biol **23:**1316–1333. http://dx.doi.org/10.1128/MCB.23.4.1316-1333.2003.
53. **Liu S, Li L, Zhang Y, Zhang Y, Zhao Y, You X, Lin Z, Zhang X, Ye L.** 2012. The oncoprotein HBXIP uses two pathways to up-regulate S100A4 in promotion of growth and migration of breast cancer cells. J Biol Chem **287:**30228–30239. http://dx.doi.org/10.1074/jbc.M112.343947.
54. **Chaki SP, Barhoumi R, Berginski ME, Sreenivasappa H, Trache A, Gomez SM, Rivera GM.** 2013. Nck enables directional cell migration through the coordination of polarized membrane protrusion with adhesion dynamics. J Cell Sci **126:**1637–1649. http://dx.doi.org/10.1242/jcs.119610.
55. **Gerhardt H, Golding M, Fruttiger M, Ruhrberg C, Lundkvist A, Abramsson A, Jeltsch M, Mitchell C, Alitalo K, Shima D, Betsholtz C.** 2003. VEGF guides angiogenic sprouting utilizing endothelial tip cell filopodia. J Cell Biol **161:**1163–1177. http://dx.doi.org/10.1083/jcb.200302047.